MAP I-2327

U.S. DEPARTMENT OF THE INTERIOR
U.S. GEOLOGICAL SURVEY

GEOLOGIC MAPS OF THE OLYMPUS MONS REGION OF MARS

By Elliot C. Morris and Kenneth L. Tanaka

Prepared for the
NATIONAL AERONAUTICS AND SPACE ADMINISTRATION

MORRIS AND TANAKA—GEOLOGY, OLYMPUS MONS REGION, MARS 1:2,000,000 AND 1:1,000,000 MAP I-2327

MISCELLANEOUS INVESTIGATIONS SERIES
Published by the U.S. Geological Survey, 1994

GEOLOGIC MAPS OF THE OLYMPUS MONS REGION OF MARS

By Elliot C. Morris and Kenneth L. Tanaka

INTRODUCTION

Olympus Mons is one of the broadest volcanoes and certainly the tallest in the Solar System. It has been extensively described and analyzed in scientific publications and frequently noted in the popular and nontechnical literature of Mars. However, the first name given to the feature—Nix Olympica (Schiaparelli, 1879)—was based on its albedo, not its size, because early telescopic observations of Mars revealed only albedo features and not topography (Inge and others, 1971). After Mariner 9 images acquired in 1971 showed that this albedo feature coincides with a giant shield volcano (McCauley and others, 1972), the name Olympus Mons was adopted for the shield to distinguish it from the albedo feature.

Olympus Mons is one of the most photographed features on the planet. The Mariner 9 spacecraft obtained 126 images of Olympus Mons with resolutions of 60 m/pixel to 2.5 km/pixel. Later, the two Viking orbiters greatly enlarged this dataset, acquiring more than 2,150 images of the Olympus Mons region at various resolutions and altitudes; 925 images have resolutions of better than 50 m/pixel. More than 150 of the Viking images provide stereoscopic coverage of the shield region (Blasius and others, 1982).

The Mariner 9 images formed the basis for the first formal geologic mapping of Olympus Mons at 1:5,000,000 scale (as part of a series of 30 quadrangles that cover the planet). Olympus Mons is included on two maps in this series (Carr, 1975; Morris and Dwornik, 1978) because of the locations of quadrangle boundaries. Viking-based 1:2,000,000-scale maps of the Tharsis region (Scott and others, 1981) that highlight lava-flow fronts also include Olympus Mons; important features of the Tharsis region are shown in figure 1 (sheet 2). More recently, the Olympus Rupes and vicinity in the southeastern part of the map area were mapped by Morris and others (1991); their map differs in detail from the current maps because of differences in interpretation. Global maps of Mars (Scott and Carr, 1978; Scott and Tanaka, 1986) place the volcano within a broader context. Finally, a special Transverse Mercator photomosaic base (fig. 2) was prepared by the U.S. Geological Survey (1981) for geologic mapping of Olympus Mons at 1:2,000,000 scale. A reduced, 1:3,000,000-scale version of this photomosaic served as the base for an informal geologic map produced as part of a thesis dissertation (Tanaka, 1983).

Our map (sheet 1) is the first formal geologic map focused on the Olympus Mons region. After compilation of this map was well underway, a 1:1,000,000-scale special topographic map of the shield area of the volcano (unpublished) was constructed from stereoscopic image pairs by using conventional photogrammetric techniques and analytical stereoplotters (see Wu and others, 1981). We were able to use this base for detailed mapping of the shield (sheet 2). The topographic map permits measurements of relief valuable in determining such factors as volcano volume, structural offsets, and lava-flow rheology. Except for the difference in extent of the areas mapped, the topographic information, the cartographic control (latitudes and longitudes of features may differ by as much as a few tenths of a degree), and the greater detail permitted by the larger scale base, the two maps are virtually the same. A comparison of our map units with those of other Viking-based maps is given in table 1.

Unraveling the geology of the Olympus Mons region is not limited to a simple exercise in stratigraphy. Complex and difficult problems arise from the unresolved origin of major geologic features that include the aureoles, the basal scarp, and the annular depression on the south and east flanks. However, our mapping does provide stratigraphic and structural evidence that assists in solving these geologic problems.

Table 1. *Comparison of map units of this and previous maps of Olympus Mons region*

This map	Scott and Tanaka (1986)	Tanaka (1983)	Scott and others (1981)
Aar, Aah, Aab, Aas	As	As	As
Amr	Ae, Amm, Amu	Aal, Aeu	Aeu
Ams	Ae, Amm, Amu	Aal, Aeu	Aeu
Amp	Ae, Amu	Aeu	Aeu
Aa_3	Aa_3	Aap_2, Apu	Aps
Aa_1	Aa_1	Aap_1	$AHoa_1$
Aoc_{1-4}	Aos	Aom_2	Aom_2
Aop	Aop	Aop, Avop	Aop
Aos_{1-4}	Aos	Aom_2	Aom_2
Aoau	Aoa_4	$AHoa_4$	Aau_4
$Aoam_a$	$Aoa_{3,4}$	$AHoa_{3,4}$	$AHoa_{3,5}$
$Aoam_b$	$Aoa_{1,3}$	$AHoa_{1,2c}$	$AHoa_{2,3}$
$Aoam_c$	Aoa_3	$AHoa_{2c}$	$AHoa_3$
$Aoam_d$	Aoa_2	$AHoa_{2b}$	$AHoa_2$
$Aoam_e$	Aoa_2	$AHoa_{2a}$	$AHoa_2$
Aoal	$Aoa_{1,2}$	$AHoa_{1,2d}$	$AHoa_2$
AHosc, HNosc	Hf	Aom_1	Aom_1, HNht
Atm, AHtm	At_4, AHt_3	Atm	Atm, Aam_3
Acf	AHcf	AHac	Acf
Aam	Aam	AHac	Aap_3
Hal	Hal	AHac	$AHap_2$
Hhf, Hhp, Hhh	v	HNvu	$AHap_1$
Hf	Hf	HNpf	HNht
Nap	Npl_2	HNpr	$AHap_1$
Nam	v	HNvu	HNht
Naf	Nf	Naf	HNht

Figure 2. Photomosaic of Olympus Mons region; forms base for sheet 1 (U.S. Geological Survey, 1981). Numbers show locations of figures cited in text.

PHYSIOGRAPHIC SETTING

The Olympus Mons region encompasses more than 3 million km² on the northwest flank of the Tharsis-Syria rise (fig. 1). The huge shield volcano and its extensive aureole deposits cover more than 1.7 million km². Olympus Mons is bordered to the south and east by an arc of lava plains 100 to 200 km wide that in low- to moderate-resolution images (150–1,000 m/pixel) appear almost featureless. Within and beyond the plains is the set of grooved aureoles that completely surround the construct, extending more than 1,000 km northwest from the center of the volcano but only 600 km to the southeast. The north edge of the aureole deposits laps onto the semicircular, faulted mountain range of Acheron Fossae, which rises more than 1,000 m above surrounding plains (U.S. Geological Survey, 1989). West of Olympus Mons are the low, smooth plains of Amazonis Planitia, which descend northward into the lowlands of Arcadia Planitia. Northeast of Olympus Mons, the terrain rises toward the broad volcano Alba Patera. To the southeast are the three large shield volcanoes of the Tharsis Montes. To the southwest are rolling plains that lap up onto densely cratered terrain of the southern hemisphere.

Olympus Mons is about 600 km across and rises more than 25 km above the surrounding plains (sheet 2). The summit is a broad, nearly flat dome more than 100 km across that slopes about 1.5° northward. The complex caldera in the northwestern part of the summit is 87x65 km across and consists of at least six coalesced collapse craters. The flanks slope away from the summit at 2° to 4°; the southwest, south, and east flanks are steepest. The upper flanks are terraced in a roughly concentric pattern; spacing between terraces ranges from 15 to 50 km. The northwest flank flattens at its base to form a gently sloping plateau almost 120 km across. Segments of the scarp surrounding the volcano have a considerable range in elevation above the basal plain: the north and northwest segments rise 8 to 10 km; the southeast segment, 4 to 5 km; and the southwest, east, and northeast segments, which are nearly buried by young lava flows, rise about 2 to 4 km.

STRATIGRAPHY

The relative ages of geologic units have been determined mainly by stratigraphic relations, supplemented where possible by crater counts made on high- to medium-resolution images (50 to 150 m/pixel; table 2). Some of the units are of regional extent and are recognized far beyond the map area. The stratigraphic relations and crater densities were used to assign the map units to stratigraphic series and systems as defined by Scott and Carr (1978) and Tanaka (1986). Where possible, map-unit symbols agree with or are modified from those used by Scott and Tanaka (1986; table 1).

NOACHIAN SYSTEM

The Noachian System consists of the oldest and most extensively modified rocks on Mars, which have a high density of degraded impact craters. In the map area, Noachian rocks are limited to outcrops associated with Acheron Fossae.

Acheron Fossae assemblage

Acheron Fossae consist of an extensive system of fault scarps and grabens that cut a broad, semicircular mountain range more than 700 km long north of Olympus Mons. The range is made up of the oldest exposed rocks in the map area, the *fractured unit of the Acheron Fossae assemblage* (unit **Naf**). The north and west margins of this range are buried by young plains material (member 3 of the Arcadia Formation), and its east edge is covered largely by lava flows from Alba Patera. The structures of Acheron Fossae generally trend parallel with the main trend of the mountains. High-resolution images (fig. 3) show the fracturing and faulting to be most intense along the east edge of the mountain range, where many sliverlike fault blocks show varied amounts of displacement. In many parts of Acheron Fossae, small dendritic and parallel sets of channels cut crater walls, ridge flanks, and hummocky areas, and many low places appear to be resurfaced by lava flows, dunes, debris aprons, and mantle deposits (figs. 3 and 4). Fields of small mesas and domes occur along the west and north margins of Acheron Fossae; many appear to be remnants of a rugged layer of weakly consolidated material that once blanketed some areas. Other domes have summit craters and may be volcanoes. These various mesas and domes are mapped as the *mountain unit of the Acheron Fossae assemblage* (unit **Nam**; fig. 5). Some mesas and domes appear to be cut by Acheron Fossae faults (fig. 5). The arcuate form of the range and its location near Olympus Mons suggest that the Acheron Fossae material may be the remnant of an old shield volcano whose central part has subsided or collapsed (Scott and others, 1981).

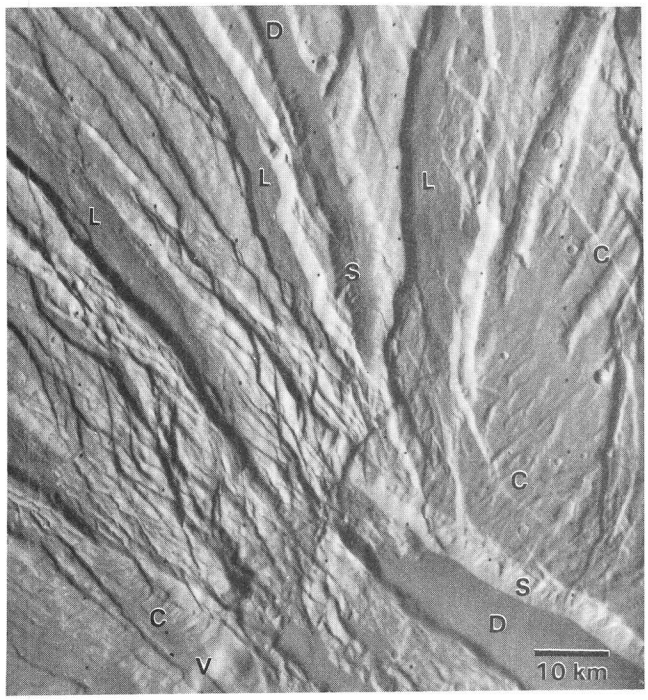

Figure 3. Part of eastern Acheron Fossae showing intense faulting in fractured unit of Acheron Fossae assemblage (unit **Naf**). Older slopes and scarps show channels (C) and spurs and gullies (S). Grabens filled by lava flows (L) or debris aprons (D). Relatively smooth hill with summit pit may be volcano (V). North at top. [Viking image 40B30]

Table 2. *Crater densities of selected map units in Olympus Mons region*

[N=number of craters whose diameters are greater than 1 km (200 m for figures in parentheses) per 10^6 km^2; σ=standard deviation, square root of cumulative number of craters divided by area]

Unit	Map-unit symbol	Cumulative no. of craters	Area (km^2)	N±σ	Reference
Rolling plains, striated members of Medusae Fossae Fm	Amr, Ams	—	—	64±20 to 510±100	1
Member 3 of Arcadia Fm	Aa_3	—	—	800	2
Member 1 of Arcadia Fm	Aa_1	—	—	500	2
Caldera member 3 of Olympus Mons Fm	Aoc_3	3	2,201	(1363±787)	3
Caldera member 2 of Olympus Mons Fm	Aoc_2	19	8,239	(2306±529)	3
Caldera member 1 of Olympus Mons Fm	Aoc_1	6	2,758	(2175±888)	3
Caldera members 1-4 of Olympus Mons Fm	Aoc_{1-4}	—	672	110	4
Plains member of Olympus Mons Fm	Aop	—	—	17±6 to 48±12	5
		13	143,200	91±25	6
		—	—	>120	4
Shield member 3 of Olympus Mons Fm	Aos_3	25	221,590	112±23	3
Shield member 2 of Olympus Mons Fm	Aos_2	14	105,110	133±36	3
Shield member 1 of Olympus Mons Fm	Aos_1	8	16,180	494±175	3
		—	1,900	400±140	7
Shield members 1-4 of Olympus Mons Fm	Aos_{1-4}	—	—	15±5 to 72±12	5
		—	243,454	27±11	8
		—	—	20 to 50	9
		25	156,400	160±32	6
		—	—	70 to 270	4
Aureole members of Olympus Mons Fm	Aoau, $Aoam_{a-e}$, Aoal	—	—	1,000 to 2,400	4
Scarp members of Olympus Mons Fm	AHosc, HNosc	2	1,180	1,700±1,200	10
Ceraunius Fossae Fm	Acf	174	123,200	1,410±110	3
Middle member of Alba Patera Fm	Aam	—	—	1,900 to 2,200	3
Lower member of Alba Patera Fm	Hal	—	—	1,800 to 2,400	11
		—	—	2,300 and 3,900	9
		—	—	2,000 to 3,500	12
		227	176,000	1,290±100	6
		—	38,860	5,020	4
		—	—	1,600	2
		—	—	2,400 to 4,000	3
Fractured plains material	Hf	—	—	3,800	9
		—	248,200	290 to 1,840	4
		—	46,227	2,400±228	13
		—	10,479	4,600±663	13
		247	116,086	2,128±135	3
Plains unit of Halex Fossae assemblage	Hhp	—	—	2,400 to 4,000	11
		116	24,296	4,774±443	3
Plains unit of Acheron Fossae assemblage	Nap	—	—	2,000 to 5,500	3
Fractured unit of Acheron Fossae assemblage	Naf	—	—	3,500 to 5,800	3

[1]Scott and Tanaka (1982)
[2]D.H. Scott, oral communication, 1982
[3]This map
[4]Hiller and others (1982)
[5]Carr and others (1977)
[6]Scott and Tanaka (1981)
[7]Blasius (1976)
[8]Plescia and Saunders (1979)
[9]Wise and others (1979)
[10]Tanaka (1983)
[11]Schaber and others (1978)
[12]Morris and Howard (1981)
[13]Plescia and Saunders (1982)

The Acheron mountain range encloses a shallow basin covered by the *plains unit of the Acheron Fossae assemblage* (unit **Nap**), which is a mantle of smooth material that appears to be draped over large impact craters. This material is marked by wrinkle ridges and may be pyroclastic or eolian. Some flows may have been erupted from the long ridge along the west edge of the basin, mapped as part of the mountain unit (fig. 6). The ridge appears to be a linear volcano, because it is cut by a crestal fissure that has been filled, presumably by volcanic material. The southern part of the plains unit is buried beneath the lower aureole and plains deposits of Olympus Mons. Although the Acheron Fossae materials have a Noachian stratigraphic position, their surfaces were somewhat modified in later periods.

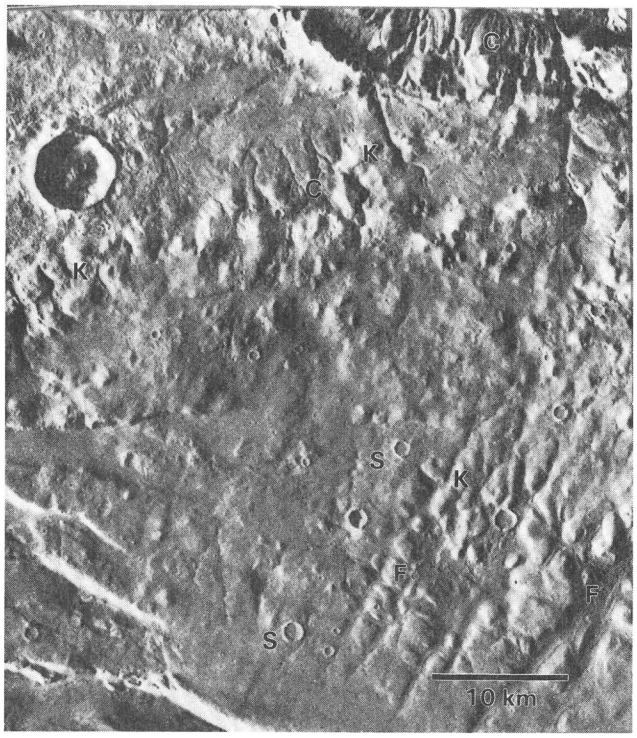

Figure 4. Ancient, complexly degraded surfaces of fractured unit of Acheron Fossae assemblage (unit **Naf**). Slopes and crater wall cut by dendritic channels (C). Mass wasting and channeling have degraded high areas into knobs (K), some of which appear associated with local fractures (F). Many crater rims are subdued (S), indicating probable mantling. North at top. [Viking image 130A29]

HESPERIAN SYSTEM

The Hesperian System consists of moderately cratered rocks whose primary morphologies are relatively well preserved. Thus, more diagnostic landforms associated with lava flows, volcanic vents, and faulting are more common than in Noachian materials. In the map area, Hesperian rocks are mostly volcanic, exposed in the scarp of Olympus Mons and in surrounding plains.

Halex Fossae assemblage

Centered at lat 27.5° N., long 126.5°, Halex Fossae consist of a series of concentric, arcuate grabens that become more closely spaced to the west (fig. 7). They probably define an old, collapsed volcanotectonic center from which flows were erupted (Schaber and others, 1978; Hodges and Moore, 1979; Plescia and Saunders, 1979). Although the structure is largely buried, radii of the arcuate fractures indicate that it may be at least 250 km across. The faulted material is mapped as the *fractured unit of the Halex Fossae assemblage* (unit **Hhf**). Lavas that appear to have flowed away from the center of Halex Fossae and that bury some of the fractures are mapped as the *plains unit* (unit **Hhp**). Hills several kilometers in diameter surrounded by flowlike features near the center of the fractured area are formed by the *hilly unit* (unit **Hhh**; fig. 7); the hills appear to be volcanoes from which small lava flows emanated.

Plains materials

Southeast of Olympus Mons, smooth plains cut by closely spaced fractures (which trend N. 45°–50° W. and N. 10°–20° W.) are formed of the *fractured plains material* (unit **Hf**). The fractures are part of the Tharsis-Syria Planum tectonic system that dominates the western hemisphere of Mars (Wise and others, 1979; Scott and Dohm, 1990). The plains were probably formed by flood lavas prior to the episode of fracturing; however, few flow fronts are observed. The fracturing may have developed prior to the main shield-building episode of the Tharsis region but possibly concurrently with postulated tectonic uplift of the region (Carr, 1975; Plescia and Saunders, 1979).

Northeast of Olympus Mons, the *lower member of the Alba Patera Formation* (unit **Hal**) forms broad, low plains made up of large sheet and tube-fed flows (Schneeberger and Pieri, 1991). Crater counts obtained on these flows have a wide range (table 2). The ejecta of some craters greater than 20 km in diameter are buried by the flows, indicating that the ejecta were emplaced on older plains material.

Scarp members of Olympus Mons Formation

As noted above, Olympus Mons is bordered by a basal scarp whose relief ranges from 2 to 10 km. Radial faults cut the scarp into segments, which form some 14 structural blocks or major sectors (Tanaka, 1983, fig. 4.1) that are partly buried by younger shield flows. Materials within these blocks are layered. Raised rims along the edge of the scarp in some of the the structural blocks suggest that the blocks are rotated down

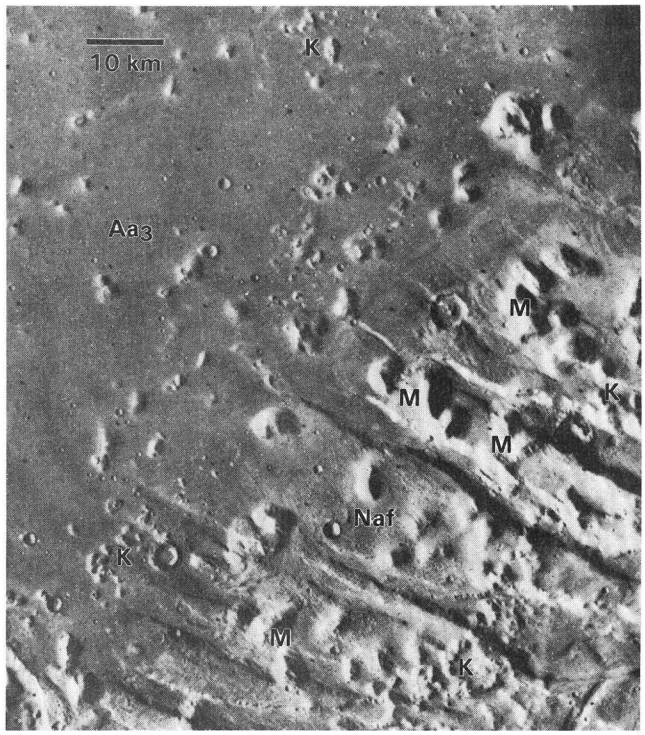

Figure 5. Northwestern part of Acheron Fossae showing fractured unit of Acheron Fossae assemblage (unit **Naf**) eroded into knobs (K), cut by grabens, and embayed by member 3 of Arcadia Formation (unit **Aa3**). Some large mountains (M) have small pit craters at their summits and may be volcanoes; they are mapped as mountain unit of Acheron Fossae assemblage (unit **Nam**). North at top. [Viking image 130A21]

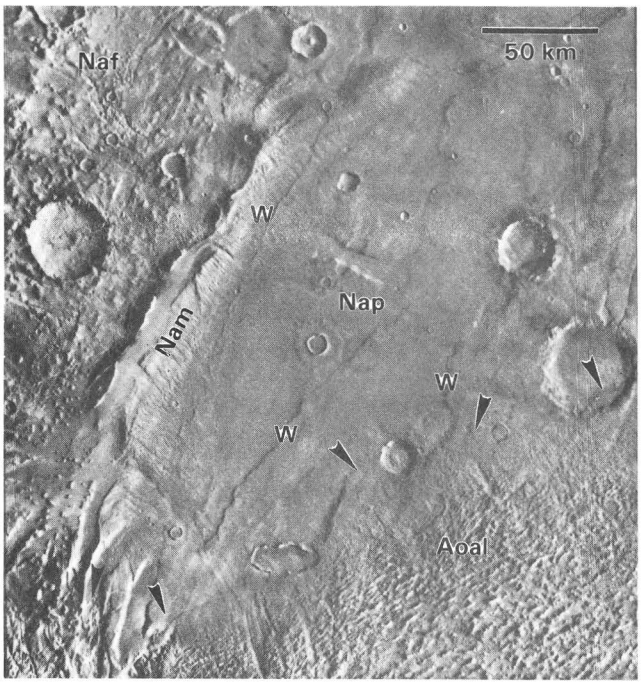

Figure 6. Part of fractured unit of Acheron Fossae assemblage (unit **Naf**) embayed by plains unit (unit **Nap**). In turn, plains unit is overlapped by lower aureole member of Olympus Mons Formation (unit **Aoal**); arrows indicate edge of aureole. Long ridge of mountain unit (unit **Nam**) has crestal rift that may be volcanic fissure. Plains unit has wrinkle ridges (W) and subdued and degraded craters. North at top. [Viking image 851A32]

toward the center of Olympus Mons. We divide the materials of the scarp into eastern and western members. The *eastern scarp member* (unit **HNosc**) forms steep cliffs and ledges. The rough upper surfaces of the structural blocks on the rim of the scarp are intensely fractured and transected by grabens (fig. 8). These upper surfaces are similar to those of the fractured plains material 300 km to the southeast, which suggests that these units may be the same material (Hiller and others, 1982). Landslides are not present along the eastern scarp. In contrast, much of the *western scarp member* (unit **AHosc**) has collapsed to form landslides of slump blocks and debris flows. The unit is capped locally by a smooth, bright layer. Where this upper layer has been eroded away, fine-scale troughs and ridges appear (fig. 9). On the north edge of Olympus Mons, a block of the western scarp member appears to be thrust over aureole middle member c (unit $\mathbf{Aoam_c}$; fig. 10). The common occurrence of landslides along the western scarp and their absence along the eastern scarp may reflect a difference in the mechanical properties of the materials or the higher shear stresses developed in the higher relief western scarp member.

AMAZONIAN SYSTEM

Amazonian rocks form the youngest materials on Mars, and thus they are superposed by relatively few impact craters. Where resistant, these rocks preserve many pristine geomorphic features. Subsequent to the extensive Hesperian Alba Patera volcanism, Amazonian eruptions deposited volcanic rocks in the Olympus Mons region from Tharsis Montes, Alba Patera, Ceraunius Fossae, fissures in Amazonis Planitia, and Olympus Mons itself. These rocks are part of the western volcanic assemblage (Scott and Tanaka, 1986), here called the Tharsis assemblage to avoid overinterpretation (that is, some units such as the Olympus Mons aureoles may include nonvolcanic materials). Other activity produced the Medusae Fossae and Arcadia Formations and landslide materials, indicating that the Amazonian Period was much more geologically active in the Olympus Mons region than elsewhere on Mars (Tanaka, 1986; Tanaka and others, 1988).

The *older member of the Tharsis Montes Formation* (unit **AHtm**) is exposed southwest of Olympus Mons where overlying layers of the Medusae Fossae Formation have been deflated by wind (fig. 11). Renewed volcanic activity east of the map area produced the *middle member of the Alba Patera Formation* (unit **Aam**) and the *Ceraunius Fossae Formation* (unit **Acf**); these units consist of sheet flows hundreds of kilometers long, a few of which extend into the plains in the northeastern part of the map area. The *younger member of the Tharsis Montes Formation* (unit **Atm**) partly buries Ulysses Fossae and easternmost outcrops of the Medusae Fossae Formation. The broad sheet flows of the unit apparently originated from areas west of Arsia Mons (fig. 1) and flowed northwestward for hundreds of kilometers, lapping onto the edge of the lowermost aureole deposit of Olympus Mons.

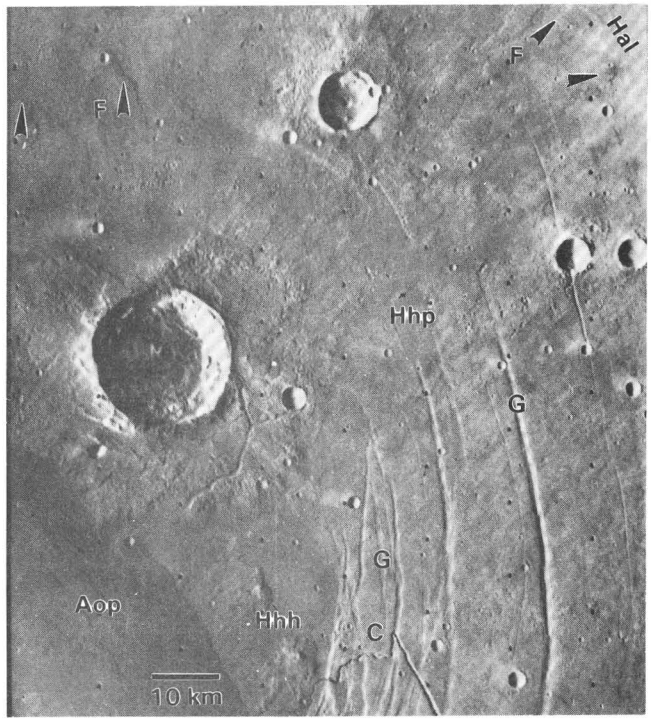

Figure 7. Arcuate grabens (G) in plains unit of Halex Fossae assemblage (unit **Hhp**) northeast of Olympus Mons. Hilly unit (unit **Hhh**) forms small hills surrounded by flows; hills are probably volcanoes. Note small (lava?) channel (C) that passes near a probable volcano and crosses several grabens. Flows (F) radiate from fossae center (arrows indicate direction of flow) and bury some grabens. Southwestern part of plains unit buried by plains member of Olympus Mons Formation (unit **Aop**), whereas northeastern part buried by lower member of Alba Patera Formation (unit **Hal**). North at top. [Viking image 43B23]

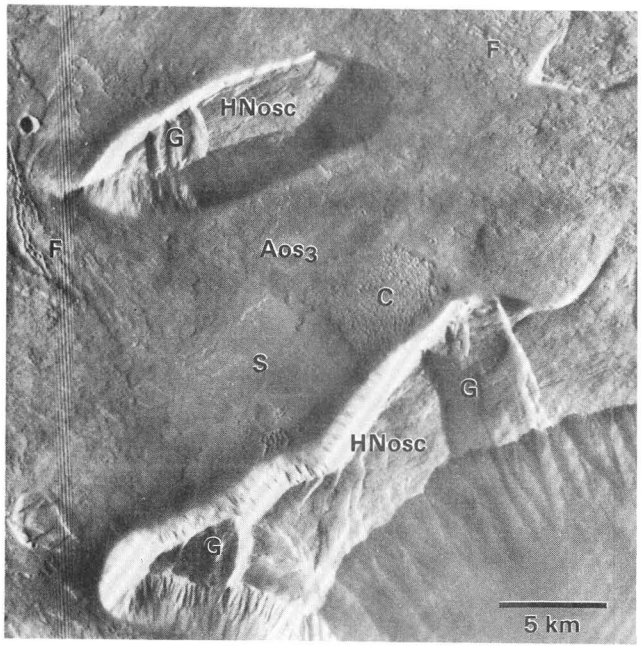

Figure 8. Blocks of eastern scarp member of Olympus Mons Formation (unit HNosc) embayed by shield member 3 (unit Aos_3) along southeastern part of scarp. Scarp materials fractured by grabens (G) and normal faults. Flows of shield member range from moderately degraded, narrow fingers (F) to broad sheets having smooth (S) or crenulated (C) surfaces; crenulations formed by large pressure ridges. North at top. [Viking image 468S64]

Olympus Mons aureole members

The aureoles of grooved terrain that surround Olympus Mons make up the most extensive unit type in the map area and one of the most remarkable features on Mars. The exposed area of the aureoles is 8.36×10^5 km^2. The aureoles consist of at least seven separate, roughly circular, overlapping sheets of material of uncertain origin (Hodges and Moore, 1979; Lopes and others, 1980, 1982; Morris, 1982; Francis and Wadge, 1983; Tanaka, 1985). The stratigraphic sequence of the aureoles is also somewhat uncertain because overlap relations among some of the units are unclear. Earlier workers suggested various sequences (table 1; see also Morris, 1982, Francis and Wadge, 1983, Tanaka, 1985); we, conservatively, divide the aureoles into *lower* (unit Aoal), *middle* (units $Aoam_{a-e}$), and *upper* (unit Aoau) *members*. The lower member clearly underlies all other members, and the upper member overlies middle members a, b, and c but does not have exposed contact with middle members d and e. Also, middle member c overlies middle member b (fig. 12).

The aureoles are characterized by curvilinear ridges and troughs 10 to 100 km long and 1 to 5 km wide that have 0.5 to 1.5 km of relief. The ridges and troughs form anastomosing patterns that differ in length and width within individual members and in scale and texture among the members; many ridges are parallel with the outer boundaries of the units. Close up, the ridges appear rugged, highly faulted, and flanked by talus slopes (fig. 13). Most individual members can be distinguished from adjacent ones by average length, width, or orientation of their ridges. The middle and upper members have larger ridges than the lower member. Most of the edge of middle member b is outlined by prominent ridges. In places, the ridge patterns are broken by sets of long, linear grooves, some of which may be eroded fracture zones of strike-slip faults (fig. 12). The grooves are confined to individual members and do not cross boundaries to lower aureoles or other units.

The lower aureole member (unit Aoal) thins toward its terminus, whereas the upper aureoles terminate in abrupt scarps or ridges. During emplacement, the lower aureole member was deflected around barriers such as crater rims, indicating flow (Carr and others, 1977; Morris, 1982). A marked difference in morphology between the lower member and the other members is evident in the smaller dimensions of its ridges and troughs. The concentric ridges of this unit appear subdued over most of its exposure, and secondary sets of radially oriented ridges and grooves have developed in many areas (fig. 14). These secondary sets have nearly obliterated the concentric structures in some places. If the secondary ridges result from local movements, their alignments are perpendicular to transport directions (Tanaka, 1985). In places, the secondary ridges have streamlined shapes and may be yardangs (McCauley, 1973; Morris, 1982). If so, they indicate that the lower member is more susceptible to erosion than the others. However, the secondary ridges of the lower member must have been developed by the time of emplacement of the upper member, which buries them. Secondary ridge structures in the middle and upper members (larger but fewer than those in the lower member) appear to be mainly related to secondary movements (Tanaka, 1985).

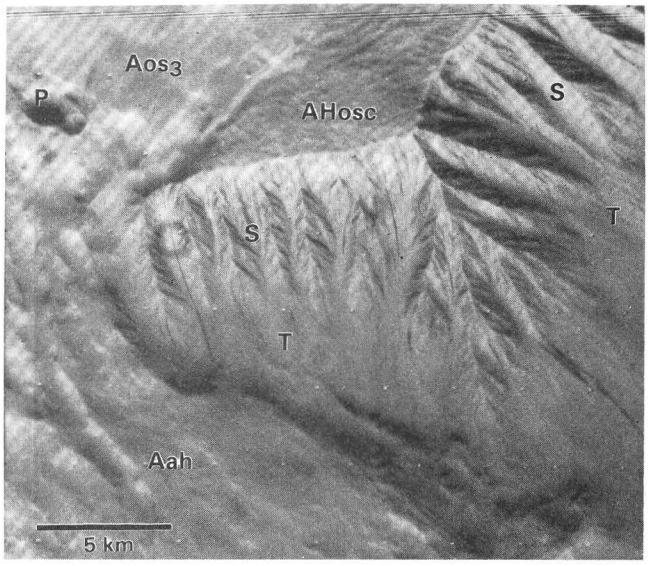

Figure 9. Block of western scarp member of Olympus Mons Formation (unit AHosc) embayed by shield member 3 (unit Aos_3) and hummocky apron material (unit Aah). Note corrugated surface of scarp member, pits (P), extensive spurs and gullies (S), and talus slope (T) along scarp. Oblique view from northwest. North at left. [Viking image 476S26]

The aureole deposits have few impact craters (Morris, 1982). Only 51 craters larger than 1 km in diameter with coherent rims have been recognized. None of these craters have mappable ejecta blankets. About an equal number of incomplete circular features that could be highly degraded impact craters are found on the aureoles. The lack of kilometer-size craters on these units relative to even younger units that embay them indicates that craters are not retained, possibly because of rapid erosion due to the aureoles' composition and rugged topography. However, larger craters are more apt to be preserved, and smaller craters (< 500 m in diameter) can be counted in selected areas. The density of craters larger than 5 km, stratigraphic relations (Scott and Tanaka, 1986; Tanaka, 1986), and counts of craters less than 1 km in diameter in selected areas (Hiller and others, 1982) suggest an Early to Middle Amazonian age.

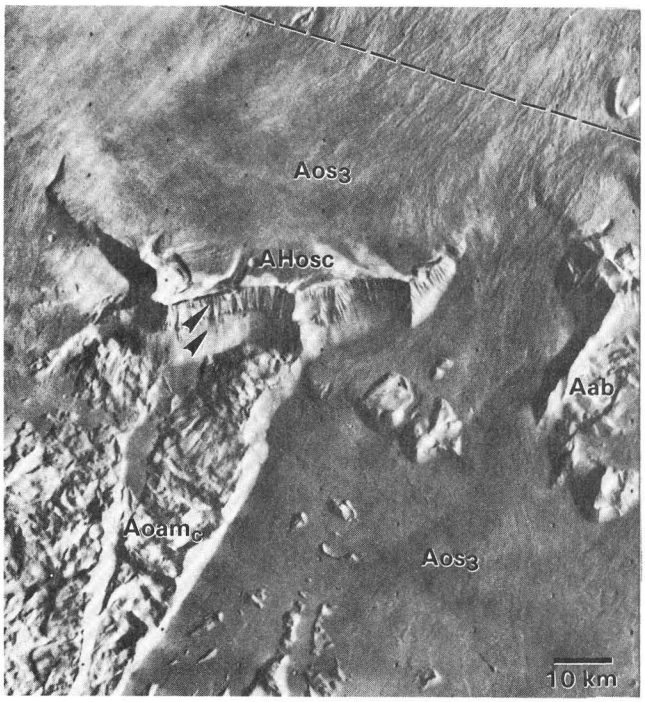

Figure 10. Section of northern scarp of Olympus Mons showing western scarp member of Olympus Mons Formation (unit AHosc) possibly thrust over middle aureole member c (unit Aoam$_c$). Scarp member shows layers (arrows) of contrasting resistance to erosion. Aureole member buried by shield member 3 (unit Aos$_3$). Dashed line shows approximate trace of fault where eastern scarp member may be thrust over western scarp member. Note blocky apron material (unit Aab) made up of several blocks of scarp material. Oblique view from north. North at bottom. [Viking image 48B14]

Olympus Mons shield members

The flanks of Olympus Mons are covered by lava flows mapped as the *shield members of the Olympus Mons Formation* (units Aos$_{1-4}$). The flows partly bury the basal scarp on the north-northeast and south-southwest sides of the shield and extend beyond the scarp as far as 170 km. Members 1–3 form extensive sequences of overlapping flows; individual flows are generally difficult to trace. Flows on the lower flanks (in units Aos$_{1,2}$) are typically long, narrow, and leveed (fig. 15); they are several hundred meters to a kilometer across and 10 to 100 km long. In some flat areas along the scarp where the flows abut high-standing outcrops of the scarp members, the flows form broad sheets; some display large pressure ridges (fig. 8). The

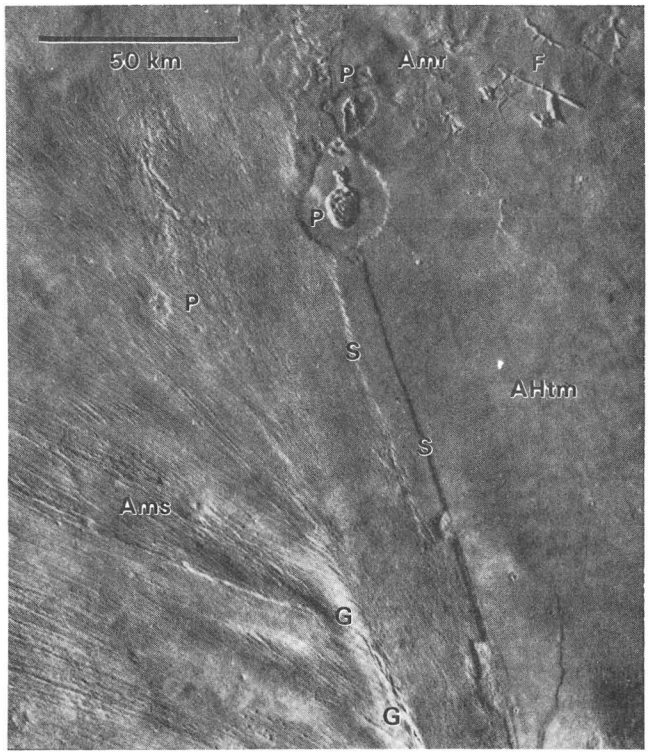

Figure 11. Plains-forming flows of older member of Tharsis Montes Formation (unit AHtm) and northern part of Gordii Dorsum (G) southwest of Olympus Mons. Striated and rolling plains members of Medusae Fossae Formation (units Ams, Amr) extensively deflated by wind. Note well-defined scarps (S) parallel to Gordii Dorsum. Serrated, pancake-shaped ejecta blankets (P) have protected underlying material from eolian erosion. Fractures and depressions (F) may be eruptive centers. North at top. [Viking image 355S03]

flows of member 3 appear relatively fresh compared with the flows on the upper flanks (unit Aos$_2$) and summit area (unit Aos$_1$). The most recent flows (unit Aos$_4$) have distinct lobate terminations and sharp boundaries and are found mostly on the south and north flanks. Flows on the upper flanks and near the summit are mostly indistinct, but some have rough, hummocky surfaces, some are stubby, and a few are broad and sheetlike. Chains and clusters of irregular to circular pit craters 100 m to 1 km in diameter occur near the summit and probably are collapsed lava tubes and vents.

Hulme (1976) inferred the composition of an Olympus Mons flow from its dimensions, morphology, slope, and a rheological model. He suggested that the lavas are more silicic than the Hawaiian basalts. Moore and others (1978) derived similar results by comparing Bingham model yield strengths of

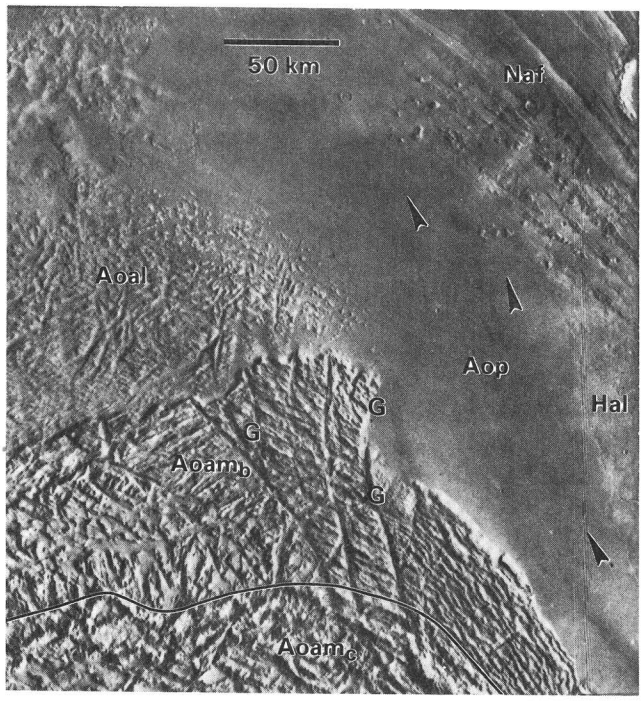

Figure 12. Area north of Olympus Mons showing overlap (line at contact) of middle aureole member c of Olympus Mons Formation (unit Aoam$_c$) on middle member b (unit Aoam$_b$), which in turn overlies lower aureole member (unit Aoal). Note differences in ridge and valley dimensions, relief, and patterns among members. Grooves (G) in middle member b are offset horizontally. Flows of plains member of Olympus Mons Formation (unit Aop; arrows indicate direction of flows) embay aureoles as well as fractured unit of Acheron Fossae assemblage (unit Naf) and lower member of Alba Patera Formation (unit Hal). North at top. [Viking image 852A08]

terrestrial and Olympus Mons flows. However, the validity of these inferences of composition has been challenged because of the complex factors involved (Baloga, 1988).

The complex nature of the flows on the flanks of Olympus Mons has hampered attempts to delineate the boundaries of the various flow sequences on the basis of morphology alone (Neal, 1981). A false-color image of Olympus Mons (sheet 2) that was processed to enhance albedo reveals recognizable differences in albedo of various parts of the shield. The summit and lower flanks are brighter than the middle flanks, although the boundaries of the albedo changes do not appear to coincide with lava flows that can be recognized in high-resolution pictures. However, because the albedo and morphologic differences of the flow units can be roughly correlated, we used albedo variations to delineate shield members 1–3. The albedo differences may be caused by thin coverings of transient eolian or pyroclastic material (Francis and Wood, 1982; Lee and others, 1982), or they may be due to compositional and weathering differences among the flows.

The local sources of most flows on the flanks of Olympus Mons cannot be identified. Carr and others (1977) suggested that most vents from which the flows originated are located on the terraced upper flanks (fig. 16). Flows on the lower flanks may have been fed primarily by long distributary systems that included leveed channels and lava tubes. Also, many lava fans are found on the lower flanks and at the foot of the basal scarp. The complex and intricate boundaries between flow sequences also indicate complex distributive systems originating along concentric scarps (figs. 15, 17), unlike the systems of Hawaiian and other terrestrial shield volcanoes that erupt mainly along rift zones radial to the central caldera (Carr and Greeley, 1980, p. 41). On the other hand, Fiske and Jackson (1972) showed that eruption from concentric fractures may be expected for isolated shields; Olympus Mons' concentric terraces are consistent with this scenario. The central caldera of Olympus Mons, though not the vent for most of the flows that streamed down the flanks, truncates flows that originated within the summit area (fig. 17). The flows possibly are older than the main caldera-forming event, or they may have issued from fissures along the rim of the caldera after it formed, similar to eruptions from the rim of the Mokuaweoweo crater of Mauna Loa, Hawaii (Carr and Greeley, 1980, p. 7).

Determinations of the impact-crater density on Olympus Mons have been attempted by various workers. Because the methods used are different and the number of impact craters available for statistical analysis is small, some variance exists among the studies. However, all are in agreement that the surface is very young and that the lower flanks appear younger than the summit area (table 2).

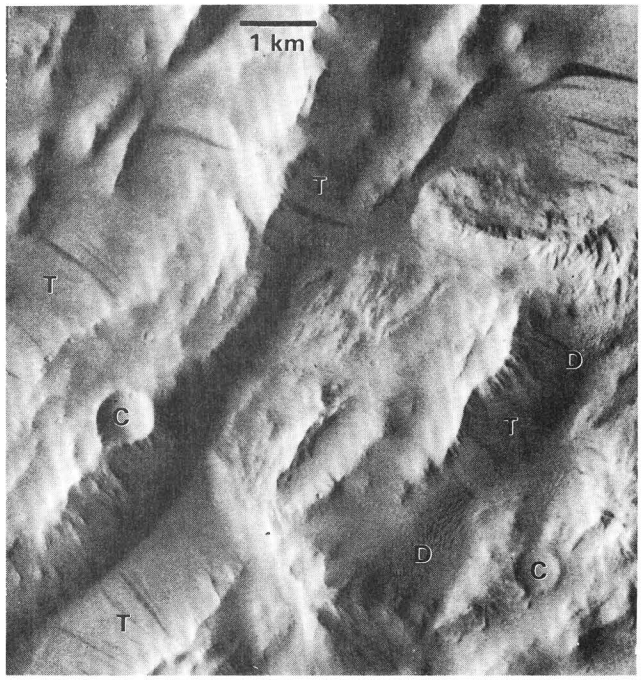

Figure 13. High-resolution image of part of upper aureole member of Olympus Mons Formation (unit Aoau). Small scarps and ridges aligned parallel and perpendicular to major ridge trend may be caused by faulting. Ridge flanks generally covered by talus (T); dark streaks in talus may be composed of dark material weathered from aureole. Dunes (D) cover some valley floors. Impact craters (C) common on ridge crests. North at top. [Viking image 441B08].

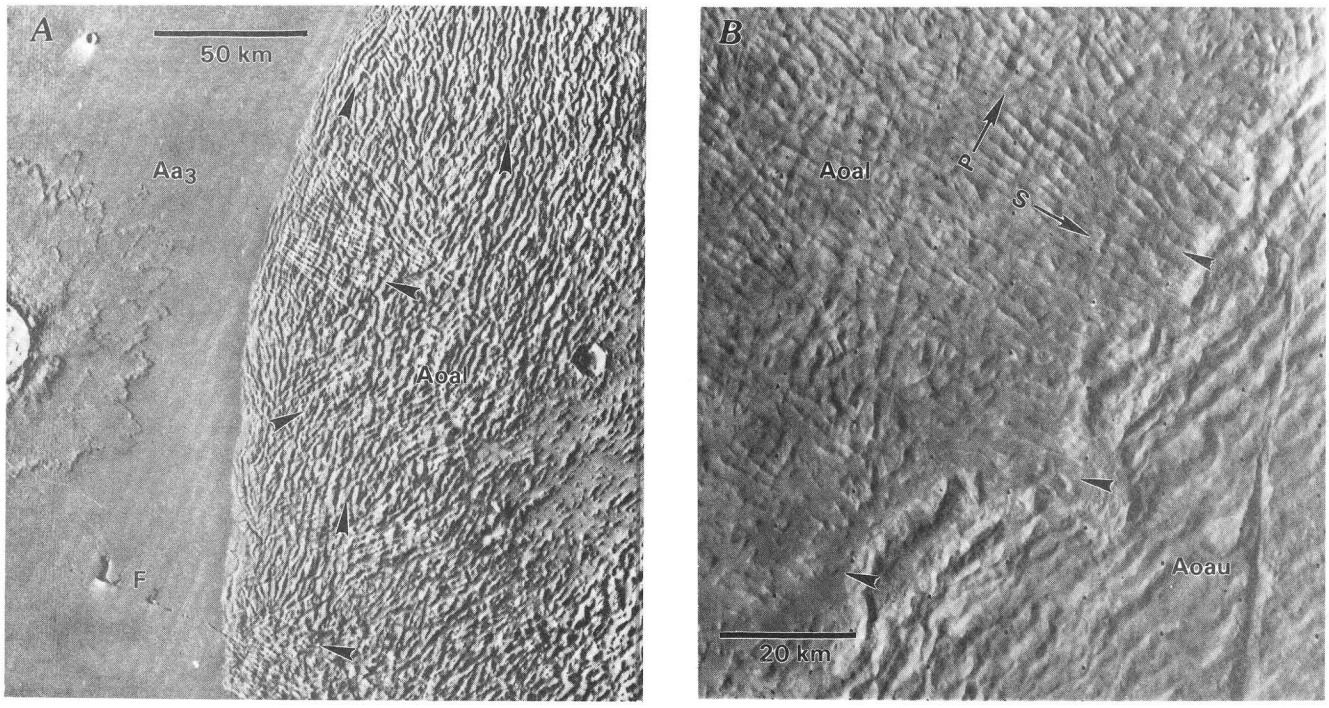

Figure 14. Ridges and valleys of lower aureole member of Olympus Mons Formation (unit **Aoal**) northwest of Olympus Mons. **A**, Aureole embayed by plains of member 3 of Arcadia Formation (unit **Aa3**). Complex sets of ridges and valleys of various orientations (arrows) developed by late-stage movements during aureole emplacement or by erosion. Fracture (F) with depressions and channels erupted lava or water. North at top. [Viking image 512A51] **B**, Lower aureole member (unit **Aoal**) overlapped by upper aureole member (unit **Aoau**). Note primary (P) and secondary (S) ridges in lower aureole; these structures were well developed prior to emplacement of upper aureole. North at top. [Viking image 45B01]

Estimating the duration of Olympus Mons' formation is problematic. If the volcano accumulated at rates comparable to those of Hawaiian volcanoes (about 0.1 km^3/yr; Swanson, 1972), it would have attained its present volume of 2.56×10^6 km^3 (Wu and others, 1981) in about 25 million years. However, Carr (1981, p. 98) considered the volcano to have developed over billions of years because of the long duration of the development of the large shields of Tharsis Montes (whose crater ages have much greater range). Although hypotheses concerning the origin of the aureoles differ greatly, the more commonly accepted ideas are that the aureoles are made of volcanic rock and may even have originated from an earlier shield. (See section on origin of the aureoles.)Therefore, the large-scale volcanism that produced the Olympus Mons Formation dates at least back to the Early Amazonian (Scott and Tanaka, 1986), a minimum of nearly 2 billion years, according to crater-flux models (Tanaka, 1986).

Olympus Mons plains member

The youngest lava flows of the Olympus Mons region flooded the plains and aureoles below the volcano's scarp on its northeast, east, and south sides, forming the relatively smooth *plains member of the Olympus Mons Formation* (unit **Aop**). Most of the unit originated from an area of fissures, circular depressions, and small, low shields in the vicinity of lat 14°–17° N., long 124°–127° (fig. 18; Tanaka, 1983); this area has also been suggested to contain sites from which ground water was released (Mouginis-Mark, 1990). The member overlaps shield member 3 of Olympus Mons in some areas; however, in other areas the shield flows may be younger. The plains member also buries several aureole members (fig. 12) and flows from Ceraunius Fossae, Alba Patera, Halex Fossae, and Arsia Mons. One patch of flows originated from an intensely fractured area of Acheron Fossae (lat 36° N., long 131°) and flowed southward, burying parts of the Acheron Fossae assemblage and Alba Patera Formation.

Olympus Mons caldera members

The complex caldera of Olympus Mons is about 10 to 20 km north of the highest part of the summit (sheet 2). The caldera is 87 km across in the northeast direction and 65 km across northwest and consists of coalesced collapse craters. Its south wall is more than 2 km high, whereas the lowest part of its north wall is only several hundred meters high (sheet 2). Its east and west rims are bordered by smooth deposits that extend several kilometers from the rims.

The caldera probably formed in a manner similar to that of large terrestrial calderas. Eaton and Murata (1960) described the formation of calderas of the Hawaiian shields as a process of cyclic intrusion of lava into a summit reservoir that causes inflation of the summit, eruption of the lava (withdrawing lava from the reservoir), and subsequent collapse of the roof of the evacuated chamber. If the Olympus Mons caldera formed by the same process (see cross section *A–A'*), at least six major collapses can be recognized within it (compare Mouginis-Mark, 1982). Other craters could have formed and been destroyed by subsequent events. After collapse the craters were filled by lava

Figure 15. Narrow flows of shield members 1 and 2 of Olympus Mons Formation (units $Aos_{1,2}$) about 40 km southeast of caldera. Some thicker flows have discernible channels with levees (arrows). Scarp (S) may be formed by thrust faulting; depression (D) may be vent for flank flows. North at top. [Viking image 475S27]

lakes; four distinct caldera-floor deposits are recognized. The oldest and largest lava lake filled the northeast half of the caldera, making up *caldera member 1* (unit Aoc_1). The solidified lava lake was downwarped, producing concentric grabens alongside and within the crater (fig. 17). The southwestern part of this deposit and part of the shield collapsed into about three coalesced craters (Mouginis-Mark, 1981) that were flooded with *caldera member 2* (unit Aoc_2). Further downwarping of caldera members 1 and 2 resulted in their overall inward-dipping floors (sheet 2) and the formation of wrinkle ridges trending dominantly northeast in the depressed caldera center (fig. 17). The ridges may have formed by squeeze-up (autointrusion) of molten lava through cracks in a cooling crust of a lava lake (Hodges, 1973; Lucchitta, 1976) or by compression and thrusting as the floor sagged due to withdrawal of lava beneath the crust of the cooling lava lake. The lava may have drained into an underlying magma chamber.

A pit crater 20 km across cuts the southwestern part of caldera member 2 (fig. 19). The smooth floor material of this crater is mapped as *caldera member 3* and is marked by a low, linear ridge across its northeast end. A narrow ridge along much of the caldera rim may represent the peak level of the now-solid lava lake that fills the crater. The member has a lower density of craters 200 m in diameter or larger than do caldera members 1 and 2 (table 2). Its elevation is slightly higher than the lowest part of member 2 (sheet 2), indicating that central downwarping of the caldera followed emplacement of member 3.

A 15-km-diameter crater cuts the northeast edge of the caldera. Fault scarps are apparent in the crater wall, and wrinkle ridges run across the crater floor (fig. 17). The floor shares with member 2 the lowest elevation within the caldera. Because the floor probably underwent less later downwarping than member 2 (as indicated by less structural modification), we surmise that this crater represents the youngest collapse event in the caldera; therefore, we mapped its floor material as *caldera member 4*. Our sequence is generally consistent with that of Mouginis-Mark (1981); the minor differences are based on the detailed topographic data.

No impact craters on the caldera floor are larger than 1 km in diameter, and most are less than 600 m. High-resolution photographs (fig. 19) show swarms of elongate and irregularly shaped secondary craters a few hundred meters in diameter on the floor of the caldera; the secondaries probably originated from an 11-km-diameter impact crater south of the caldera. This impact may have dislodged material from the caldera's rim, resulting in a small landslide (see fig. 19, not mapped; Mouginis-Mark, 1981).

Other plains materials

Plains-forming materials of the Arcadia and Medusae Fossae Formations (Scott and Tanaka, 1986) embay or bury extensive areas of aureole material and the Tharsis Montes Formation south, west, and north of Olympus Mons. Stratigraphic relations show that these plains materials are Amazonian in age; their morphologies indicate a variety of rock types.

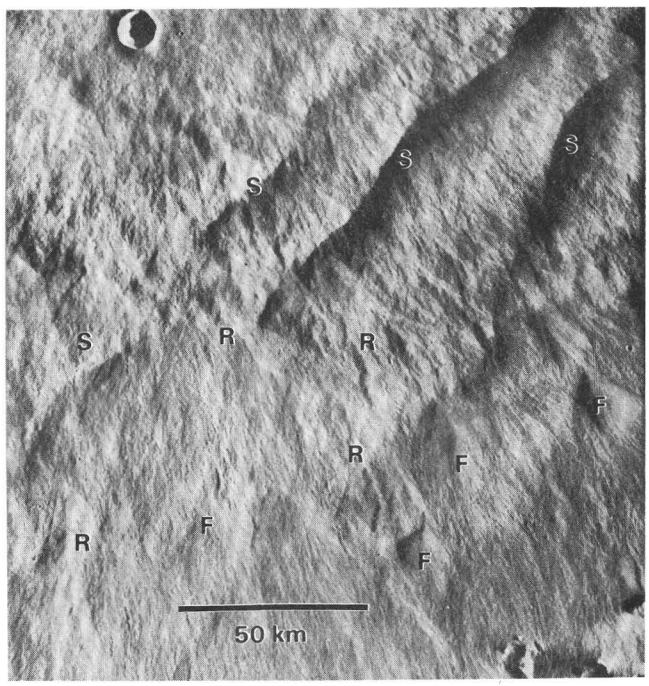

Figure 16. Part of south flank of Olympus Mons where scarps (S) possibly formed by thrust faulting are partly buried by lava flows. Scarps generally cut shield members 1 and 2 of Olympus Mons Formation (units $Aos_{1,2}$; see maps) and are buried by members 3 and 4. Some flows make up irregular ridges (R) and fans (F) that may be formed by local, voluminous eruptions originating from buried faults. North at top. [Viking image 890A70]

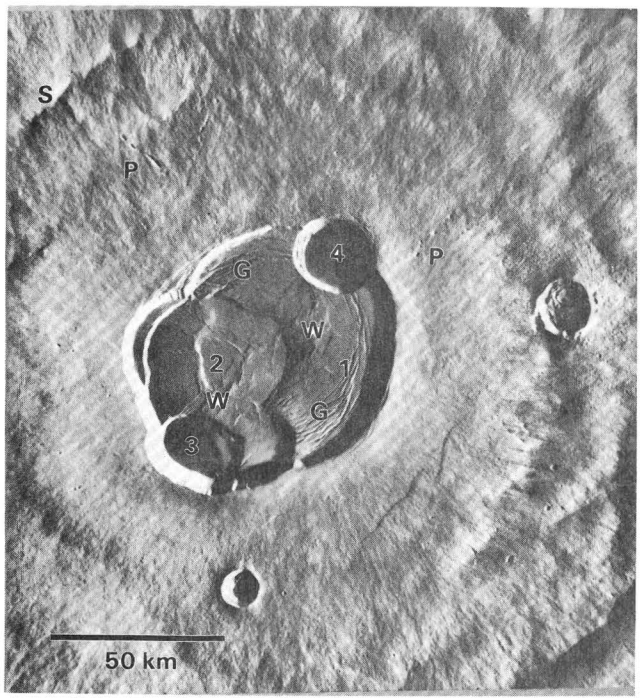

Figure 17. Caldera of Olympus Mons showing four main stages of collapse and lava-lake formation (1–4, corresponding to units Aoc_{1-4}) demonstrated by crosscutting and topographic relations. Collapse continued following lava-lake solidification in each event, as shown by warped topography of some crater floors (see sheet 2) and their concentric grabens (G) and complex wrinkle ridges (W). Note that floors 1 and 2 each fill two coalesced craters of about the same age. Surrounding caldera, pits (P) are probable vent areas, and scarps (S) may be caused by thrust faulting. Note that caldera rim cuts shield flows that radiate from caldera area. North at top. [Viking image 890A68]

Occurring northwest of the aureoles of Olympus Mons in Amazonis Planitia, *member 1 of the Arcadia Formation* (unit Aa_1) consists of rough and dissected flows with lobate scarps. *Member 3 of the Arcadia Formation* (unit Aa_3) forms smooth plains mostly in the western part of the map area and embays member 1 and the west edge of the lower aureole member of the Olympus Mons Formation. Although the two Arcadia members are relatively featureless in medium-resolution images (except for a few lava-flow fronts), a mantle of giant ripples can be observed in high-resolution images (50 m/pixel). This mantle may consist of a mixture of eolian particles (fig. 20; Breed and others, 1987).

Members of the Medusae Fossae Formation, distinguished by morphology, are the *pitted* (unit Amp), *striated* (unit Ams), and *rolling plains* (unit Amr) *members.* Along the south margin of Amazonis Planitia, the formation thickens considerably and laps onto densely cratered terrain (southwest of the map area). The materials have been proposed to be pyroclastic rocks (Scott and Tanaka, 1982), paleopolar deposits (Schultz and Lutz, 1988), or some other type of eolian deposit (Greeley and Guest, 1987). Alternatively, they may be derived from erosion and redeposition of aureole materials.

South of Olympus Mons, the pitted member commonly crops out where the Medusae Fossae Formation overlies the lower aureole member. The pits are crescent shaped (fig. 21), probably eolian features (blowouts) similar to fuljis of the Arabian deserts on Earth (Rhodes and Neal, 1981). The outcrops of the member form an east-northeast-trending serrated pattern subparallel to local striations; the pattern may reflect a paleowind direction.

The striated member is made up of layers of easily eroded, striated material. It covers aureole members and Tharsis lava flows south of Olympus Mons, where its surfaces are broad and rolling. West of Olympus Mons, it fills shallow depressions in the lower, middle (unit $Aoam_a$), and upper aureole members. The striations appear to be streamlined ridges and grooves, similar to terrestrial yardangs (McCauley, 1973; Ward, 1979). Their various orientations indicate control both by prevailing wind directions and by joint patterns (Scott and Tanaka, 1982). Eroded superposed impact craters have pancake-shaped ejecta blankets with serrated edges, which indicate that the ejecta are more resistant to erosion than the underlying member.

The rolling plains member is exposed southwest of Olympus Mons (fig. 22), where it locally overlies aureole material and lava flows of the Arcadia and Tharsis Montes Formations. In some areas it grades into, in other areas it overlies the striated member. Many exposures are erosional remnants of a more extensive deposit. Some roughly circular outcrops having large irregular central pits or depressions may be volcanic vents or remnants of pancake impact craters (figs. 11 and 22).

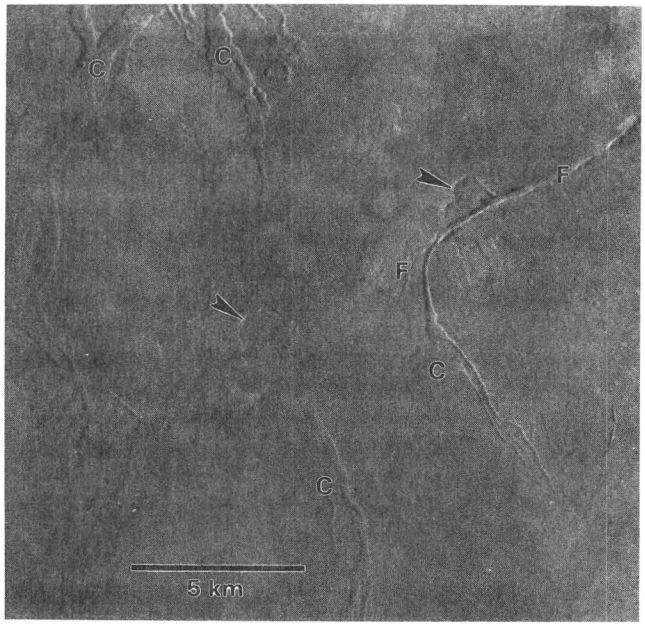

Figure 18. Volcanic plains east of Olympus Mons composed of plains member of Olympus Mons Formation (unit Aop). Channels (C) emanating from fractures (F) may be formed by volcanic flows or catastrophic discharge of ground water. Note arcuate ridges along fractures (arrows). North at top. [Viking image 468S52]

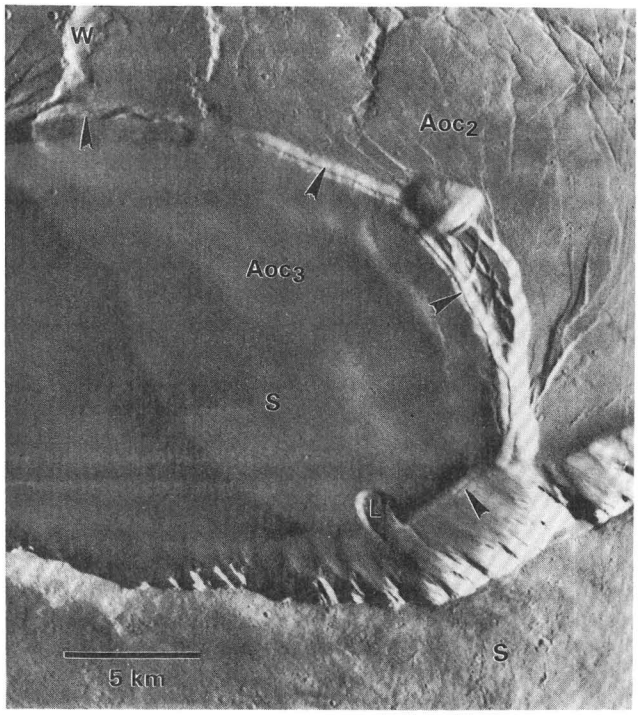

Figure 19. Southwestern part of Olympus Mons caldera showing 20-km-diameter crater filled by caldera member 3 of Olympus Mons Formation (unit Aoc3). Bench along crater wall (arrows) represents high-level mark of lava lake that filled crater. Small landslide (L) may have been triggered by impact that produced 11-km-diameter crater about 25 km to south, which also formed secondary craters (S) across shield and caldera floor. Wrinkle ridge (W) offsets crater wall. Northeast at top. [Viking image 473S03]

Apron materials

In the Olympus Mons region, aprons can be classified as four morphologic types: smooth, blocky, hummocky, and ridged. Aprons are common along the west scarp of Olympus Mons (fig. 23).

In Acheron Fossae, *smooth apron material* (unit **Aas**) covers fault scarps and crater walls and adjacent plains and valleys. Deposits apparently formed by periglacial mass wasting, as all are north of lat 35° N., within the Martian climate zone where many probable periglacial features are observed (Squyres and Carr, 1986).

Blocky apron material (unit **Aab**), found along the northern part of the scarp (fig. 10), is made up of several blocks or hummocky masses as large as 25 km across. The blocks are largely disrupted, and some have transverse ridges. These blocks were probably detached from the scarp by rotational and translational movements (Tanaka, 1982).

Hummocky apron material (unit **Aah**) is characterized by hummocky surfaces at the heads and centers of broad, lobate aprons. The morphology of the aprons is similar to that of terrestrial debris flows and piedmont glaciers (Lucchitta, 1981). Melting of ground ice may have aided the disintegration of the scarp. Lucchitta (1981) suggested that considerable ice was involved in the flows, because their terminal ridges transgress the aureole ridges without deflection and appear to be superposed on the ridges.

Two large sections of the west scarp, 50 and 100 km across, appear to have collapsed and flowed out onto the adjacent plain for more than 100 km. These relatively smooth areas of the aprons that make up the *ridged apron material* (unit **Aar**) have long, continuous, curvilinear ridges that are subparallel to the margin of the aprons. Near the scarp, the unit grades into hummocky apron material.

STRUCTURE AND TECTONICS

The intense faulting of Acheron Fossae north of Olympus Mons represents the oldest tectonic episode recorded in the map area. The grabens of the northern part of Acheron Fossae trend due west to N. 70° W., whereas those of the eastern and southeastern parts mostly trend N. 30°–40° W. and transect the more westerly faults. The northern faults are buried by the Acheron Fossae plains member and superposed by most large impact craters, indicating a Middle Noachian age for the faulting (Tanaka, 1986). It may have been associated with the collapse of an ancient volcanic center (Scott, 1982). Another possibility is that local uplift and extension (or rifting) produced the fault sets.

The eastern faults are less degraded by channeling and mass wasting than the northern faults and may be Late Noachian in age, predating the Acheron Fossae plains member. The faults parallel some of the faults of Ulysses Fossae and are radial to the Tharsis rise to the southeast just outside the map area. This faulting therefore may have developed due to stresses caused by Tharsis tectonic activity (Wise and others, 1979; Plescia and Saunders, 1982; Solomon and Head, 1982), much of which occurred in Late Noachian and Early Hesperian time (Tanaka and Davis, 1988; Scott and Dohm, 1990).

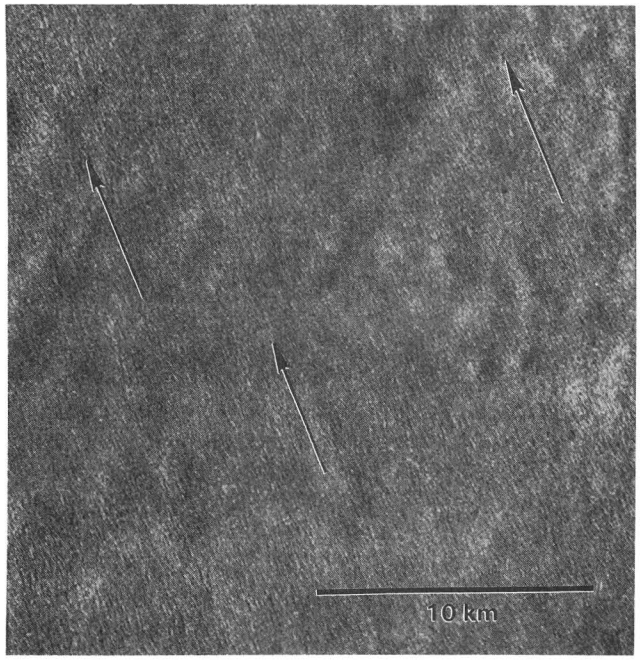

Figure 20. Giant ripples (fine linear pattern) on rolling plains made up of mantle of eolian material on member 3 of Arcadia Formation (unit Aa3) in Arcadia Planitia; arrows indicate trend of ripples. North at top. [Viking image 111A28]

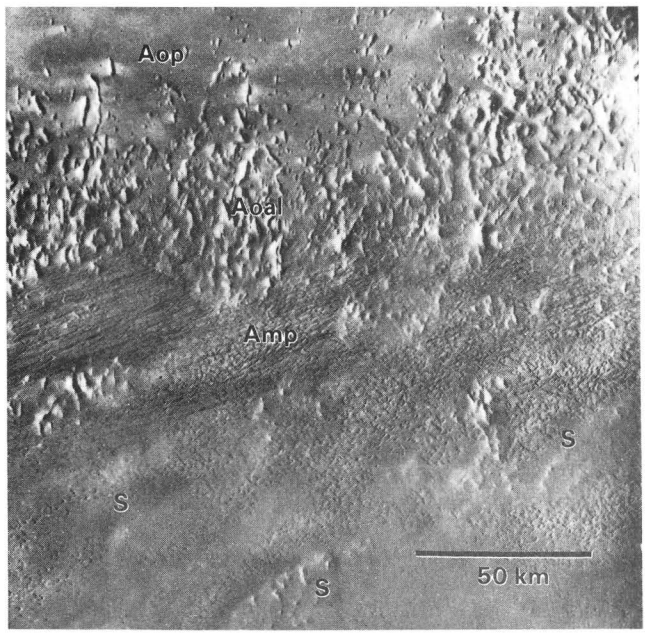

Figure 21. Pitted member of Medusae Fossae Formation (unit **Amp**) and plains member of Olympus Mons Formation (unit **Aop**) burying ridges and knobs of lower aureole member of Olympus Mons Formation (unit **Aoal**) south of Olympus Mons. Pits have crescentic shapes that indicate eolian erosion. Some arms of pits are elongated, forming striations transitional to those in striated member of Medusae Fossae Formation. Smooth areas (S) commonly associated with knobs of aureole material may be thin eolian deposits. North at top. [Viking image 44B20]

When the Halex Fossae materials were emplaced, Acheron Fossae faulting had ceased. Halex Fossae are concentric faults that apparently have a local volcanotectonic origin. They must be at least Early Hesperian in age, because they are buried by the lower member of the Alba Patera Formation. A few younger, north-trending faults of Alba Fossae cut Halex Fossae and Alba Patera materials and probably are related to Early Amazonian faulting centered at Alba Patera (Tanaka, 1990).

The age of formation of the basal scarp of Olympus Mons is somewhat uncertain. It is clearly older than the Middle and Upper Amazonian shield flows that bury it in places; however, its age relative to the aureoles is model dependent. Among various theories proposed for the formation of the scarp, two tectonic origins commonly advocated are (1) thrusting (see cross section *A–A′*; Harris, 1977; Morris, 1981; Borgia and others, 1990) and (2) detachment of lower flanks of the shield, in conjunction with a gravity sliding or spreading origin of the aureoles (Lopes and others, 1980, 1982; Francis and Wadge, 1983; Tanaka, 1985).

We interpret that, following emplacement of the aureoles, the load of Olympus Mons produced an annular basin on the southeast flank of the volcano. Distal parts of some aureole members (units **Aoal**, Aoam_d, and Aoam_e) form topographic highs (sheet 2), indicating that proximal parts are downwarped. Recent plains flows (unit **Aop**) filled the depression that had formed. Circumferential grabens would be expected with subsidence; none are seen, but some could be buried by the plains member of the Olympus Mons Formation. If no downwarp occurred, stress models indicate that the lithosphere would be at least 200 km thick—much thicker than at Tharsis and Elysium Mons (Comer and others, 1985). (Elysium Mons is centered at lat 25° N., long 213°.)

Above the basal scarp, lower flanks of the shield are partitioned by radially oriented scarps. The scarps may indicate faults along which horizontal and vertical offsets occurred between blocks of shield material. On the upper flanks, concentric terraces may have been produced by thrust faulting (cross section *A–A′*; Morris, 1981), consistent with a finite-element deformation model (Thomas and others, 1990). The terraces, radial faults, basal scarp, and annular moat around Olympus Mons were formed contemporaneously, which raises the possibility that their deformations are interrelated and attributable to loading and relaxation of the shield and the underlying lithosphere.

The craters making up the caldera of Olympus Mons resulted from collapse due to withdrawal of magma from an underlying chamber. Numerical-model studies that predict stress distributions (Zuber and Mouginis-Mark, 1990) indicate that that the top of the magma chamber is about 8 to 16 km below the summit (cross section *A–A′*).

The north end of Gordii Dorsum forms an escarpment trending N. 25° W. in the southwestern part of the map area. Although interpreted by Forsythe and Zimbelman (1989) as an ancient (Noachian-Lower Hesperian) exhumed transcurrent fault, it cuts Amazonian rocks of the Medusae Fossae and Tharsis Montes Formations, and horizontal offsets are not seen. We therefore think that Gordii Dorsum is most likely the expression of a normal fault of Amazonian age.

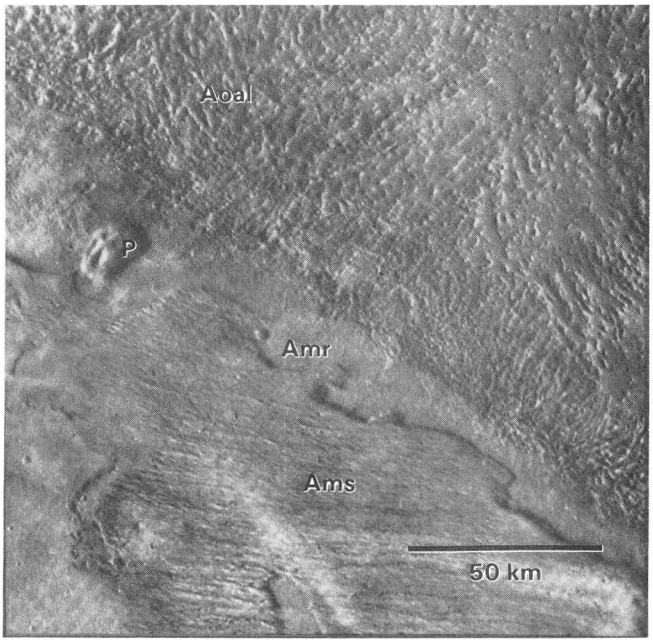

Figure 22. Relatively smooth rolling plains member of Medusae Fossae Formation (unit **Amr**) eroded away to expose striated member (unit **Ams**). These units embay lower aureole member of Olympus Mons Formation (unit **Aoal**). Oblong pit (P) may be highly eroded impact crater or volcanic vent. North at top. [Viking image 355S09]

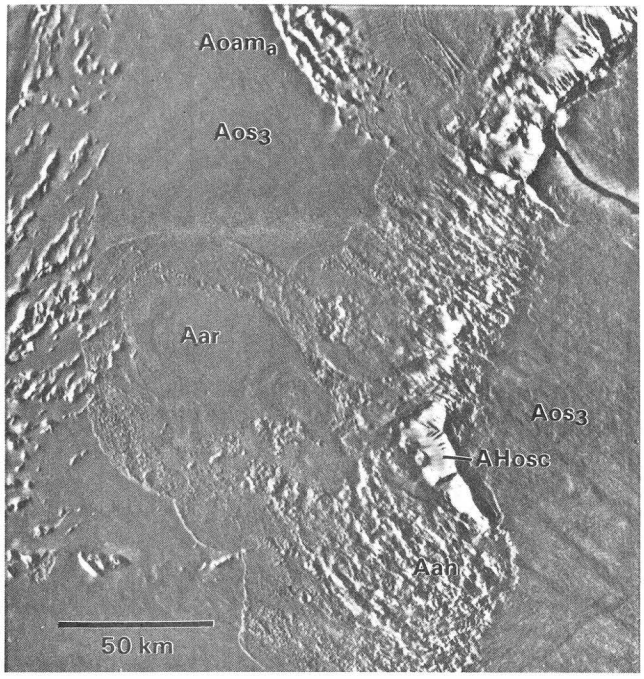

Figure 23. Lobate apron materials along west edge of Olympus Mons interpreted to be landslides derived from western scarp member (unit AHosc) and shield member 3 (unit Aos$_3$) of Olympus Mons Formation. Apron materials bury shield flows and parts of middle aureole member a (unit Aoam$_a$). Distal apron material is smooth and concentrically ridged (unit Aar), whereas apron material near scarp is rough, hummocky, and locally pitted (unit Aah). North at top. [Viking image 512A63]

ORIGIN OF THE OLYMPUS MONS AUREOLES

Each of the various origins that have been proposed for the aureoles implies different relations between them and Olympus Mons. The aureoles have been considered to be (1) deeply eroded lava flows from Olympus Mons or from earlier volcanoes (McCauley and others, 1972; Morris and Dwornik, 1978); (2) eroded remnants of older volcanic shields (Carr, 1973); (3) thrust sheets caused by the weight of Olympus Mons on layered deposits (Harris, 1977); (4) the result of subglacial eruption of lavas (Hodges and Moore, 1979); (5) landslides from the scarp surrounding Olympus Mons (Lopes and others, 1980, 1982); (6) pyroclastic deposits (Morris, 1982); and (7) deformed materials resulting from gravity spreading of the outer reaches of the Olympus Mons shield (Francis and Wadge, 1983; Battistini, 1985; Tanaka, 1985). The landslide and gravity-spreading mechanisms require a two-stage growth of Olympus Mons: first, an ancient shield formed whose flanks collapsed to form the aureoles, and second, the present shield developed on those older structures.

The first four proposals have serious difficulties that subsequent research has brought to light; their problems have been reviewed by Morris (1982) and Francis and Wadge (1983). Therefore, we consider here only hypotheses involving the pyroclastic deposits and landsliding and gravitational spreading, which we favor.

Both of the hypotheses account for many of the observed characteristics of the aureoles, such as (1) their great size and continuity, (2) their susceptibility to erosion, (3) their gross morphologic characteristics that indicate flow, and (4) the large positive gravity anomaly that extends from Olympus Mons northwestward over the largest exposure of aureole material (Sjogren, 1979). Weaknesses in each hypothesis include the need for speculation in the explanation of the flow mechanism and source. The pyroclastic hypothesis does not readily explain the lack of calderas from which the aureoles would have erupted (see Francis and Wadge, 1983). On the other hand, this hypothesis does explain the circular form of the aureoles (particularly the upper member, whose center is about 200 km from the scarp) and their concentric pattern of ridges. The landsliding and gravity-spreading mechanisms require a lubricant such as water or ice (Tanaka, 1985); also, the volumes of the aureoles east of the volcano are smaller than the expected volume of missing material below the scarp, given the scarp height (Morris, 1987). If a huge, proto-Olympus Mons had formed (necessary for the landsliding and gravity-spreading mechanisms), extant lava-flow fields beyond the aureoles might be expected, but they are absent. However, the landsliding and gravity-spreading mechanisms can account for the large size of the ridges and troughs and the orientation of the fractures (that generally indicate flow away from the scarp, rather than from aureole centers).

GEOLOGIC SUMMARY

Olympus Mons is impressive in structural complexity and in size—the tallest mountain and largest volcanic shield known to man—and it poses difficult problems debated by volcanologists, structural geologists, and geophysicists. The geologic events recorded in the rocks of the Olympus Mons region cover a major portion of Martian time—about 4 billion years. (The following discussion reflects the Hartmann-Tanaka model ages discussed in Tanaka, 1986.) The oldest rocks make up the densely cratered terrains of Acheron Fossae, which cut a broad, arcuate ridge that was a volcanotectonic center about 3.5 to 4.0 b.y. ago. During the next billion years, volcanic activity spread to centers at Halex Fossae, Alba Patera, and other local sites. This activity probably resurfaced much of the map area, but only a few outcrops of lava plains remain from this period. Over the next 2.5 billion years, voluminous lava flows and fields were emplaced sporadically from Alba Patera, Ceraunius Fossae, the three large Tharsis shield volcanoes, Olympus Mons, and other local sources. These outpourings resulted in broad, flat sheet flows that cover the plains east and west of Olympus Mons.

The aureoles of Olympus Mons, about 1.5 b.y. old, may be the result of great pyroclastic eruptions that preceded the growth of Olympus Mons, or they may be landslide or gravity-spreading features that formed on the flanks of an early, huge proto-Olympus Mons shield. The smooth, flat to gently rolling plains of the Medusae Fossae Formation south of Olympus Mons, which are locally superposed on the aureoles, may consist of pyroclastic deposits and eolian material derived from the aureoles. Amazonis Planitia, west of the aureoles, is also covered with a variety of plains-forming materials of the Arcadia Formation, including lava flows and eolian mantles; these materials are either contemporaneous with or somewhat younger than the aureoles.

Beginning perhaps as early as the earliest aureole formation and continuing to about 500 m.y. ago, the great mass of the volcano caused (1) sagging of the lithosphere that produced an annular depression on the south and east sides of the volcano and (2) circumferential thrust faulting, resulting in concentric terraces, the basal scarp, and radial faults above the scarp. Following this deformation, lava flows were erupted over the shield and at the east base of Olympus Mons, filling the annular depression. Many of the shield flows contain leveed channels or lava tubes; their morphology and inferred rheologic properties are similar to those of basaltic flows on Earth. In places along the northwestern part of the shield, the immense basal scarp collapsed to form massive slides and slumps. Within the past 100 m.y., a series of collapse events and lava eruptions at the summit of Olympus Mons produced the volcano's caldera complex of nested craters with lava-lake floors. Some lava flows on or adjacent to Olympus Mons appear on available images to be devoid of impact craters, indicating that volcanic activity has occurred within the past few million years. We should therefore not be too surprised if Olympus Mons were to resume its volcanic activity in the future.

ACKNOWLEDGMENTS

We thank Henry J. Moore of the U.S. Geological Survey and Andrea Borgia of the Jet Propulsion Laboratory for their expert reviews of this map. Several student assistants contributed to the mapping.

REFERENCES CITED

Baloga, S.M., 1988, A review of quantitative models for lava flows on Mars, *in* MEVTV Workshop on Nature and Composition of Surface Units on Mars, LPI Technical Report 88-05: Houston, Lunar and Planetary Institute, p. 17-19.

Battistini, René, 1985, Les volcans du dome des Tharsis (Mars), comparaison avec les volcans terrestres [Volcanoes of the Tharsis dome (Mars), comparison with terrestrial volcanoes]: Revue de Geomorphologie Dynamique, v. 34, no. 3, p. 81-109.

Blasius, K.R., 1976, The record of impact cratering on the great volcanic shields of the Tharsis region of Mars: Icarus, v. 29, no. 3, p. 343-361.

Blasius, K.R., Vetrone, A.V., Lewis, B.H., and Martin, M.D., 1982, Viking Orbiter stereo imaging catalog: National Aeronautics and Space Administration Contractor Report 3501, 404 p.

Borgia, Andrea, Burr, Jeremia, Montero, Walter, Morales, L.D., and Alvarado, G.E., 1990, Fault-propagation folds induced by gravitational failure and slumping of the central Costa Rica volcanic range: Implications for large terrestrial and Martian volcanic edifices: Journal of Geophysical Research, v. 95, no. B9, p. 14,357-14,382.

Breed, C.S., McCauley, J.F., and Davis, P.A., 1987, Sand sheets of the eastern Sahara and ripple blankets on Mars, *in* Frostick, L., and Reid, I., eds., Desert sediments: Ancient and modern: Geological Society of America Special Publication no. 35, p. 337-359.

Carr, M.H., 1973, Volcanism on Mars: Journal of Geophysical Research, v. 78, no. 20, p. 4049-4062.

_____ 1975, Geologic map of the Tharsis quadrangle of Mars: U.S. Geological Survey Miscellaneous Investigations Series Map I-893, scale 1:5,000,000.

_____ 1981, The surface of Mars: New Haven and London, Yale University Press, 232 p.

Carr, M.H., and Greeley, Ronald, 1980, Volcanic features of Hawaii, a basis for comparison with Mars: National Aeronautics and Space Administration Special Publication 403, 211 p.

Carr, M.H., Greeley, Ronald, Blasius, K.R., Guest, J.E., and Murray, J.B., 1977, Some martian volcanic features as viewed from the Viking orbiters: Journal of Geophysical Research, v. 82, no. 28, p. 3985-4015.

Comer, R.P., Solomon, S.C., and Head, J.W., 1985, Mars—Thickness of the lithosphere from the tectonic response to volcanic loads: Reviews of Geophysics, v. 23, no. 1, p. 61-92.

Eaton, J.P., and Murata, K.J., 1960, How volcanoes grow: Science, v. 132, no. 3432, p. 925-938.

Fiske, R.S., and Jackson, E.D., 1972, Orientation and growth of Hawaiian volcanic rifts: The effect of regional structure and gravitational stresses: Proceedings of the Royal Society of London, A., v. 329, p. 299-326.

Forsythe, R.D., and Zimbelman, J.R., 1989, The transcurrent fault hypothesis for Mars' Gordii Dorsum escarpment, *in* MEVTV Workshop on Tectonic Features on Mars, LPI Technical Report 89-06: Houston, Lunar and Planetary Institute, p. 30-32.

Francis, P.W., and Wadge, Gerald, 1983, The Olympus Mons aureole: Formation by gravitational spreading: Journal of Geophysical Research, v. 88, no. B10, p. 8333-8344.

Francis, P.W., and Wood, C.A., 1982, Absence of silicic volcanism on Mars: Implications for crustal composition and volatile abundance: Journal of Geophysical Research, v. 87, no. B12, p. 9881-9889.

Greeley, Ronald, and Guest, J.E., 1987, Geologic map of the eastern equatorial region of Mars: U.S.Geological Survey Miscellaneous Investigations Series Map I-1802-B, scale 1:15,000,000.

Harris, S.A., 1977, The aureole of Olympus Mons, Mars: Journal of Geophysical Research, v. 82, no. 20, p. 3099-3107.

Hiller, K.H., Janle, Peter, Neukum, G.P.O., Guest, J.E., and Lopes, R.M.C., 1982, Mars: Stratigraphy and gravimetry of Olympus Mons and its aureole: Journal of Geophysical Research, v. 87, no. B12, p. 9905-9915.

Hodges, C.A., 1973, Mare ridges and lava lakes, *in* Apollo 17 Preliminary Science Report: National Aeronautics and Space Administration Special Report 330, p. 31-12 to 31-21.

Hodges, C.A., and Moore, H.J., 1979, The subglacial birth of Olympus Mons and its aureole: Journal of Geophysical Research, v. 84, no. B14, p. 8061-8074.

Hulme, Geoffrey, 1976, The determination of the rheological properties and effusion rate of an Olympus Mons lava: Icarus, v. 27, no. 2, p. 207-213.

Inge, J.L., Capen, C.F., Martin, L.J., and Thompson, D.T., 1971, Mars—1971 [albedo map]: Flagstaff, Ariz., Lowell Observatory, scale 1:25,000,000.

Lee, S.W., Thomas, P.C., and Ververka, Joseph, 1982, Wind streaks in Tharsis and Elysium: Implications for sediment transport by slope winds: Journal of Geophysical Research, v. 87, no. B12, p. 10,025–10,041.

Lopes, R.M.C., Guest, J.E., Hiller, K.H., and Neukum, G.P.O., 1982, Further evidence for a mass movement origin of the Olympus Mons aureole: Journal of Geophysical Research, v. 87, no. B12, p. 9917–9928.

Lopes, R.M.C., Guest, J.E., and Wilson, C.J., 1980, Origin of the Olympus Mons aureole and perimeter scarp: The Moon and the Planets, v. 22, no. 2, p. 221–234.

Lucchitta, B.K., 1976, Mare ridges and related highland scarp—Result of vertical tectonism? *in* Lunar and Planetary Science Conference, 7th, Houston, March 15–19, 1976, Proceedings: Pergamon Press, v. 3, p. 2761–2782.

_____ 1981, Mars and Earth: Comparison of cold-climate features: Icarus, v. 45, no. 2, p. 264–303.

McCauley, J.F., 1973, Mariner 9 evidence for wind erosion in the equatorial and mid-latitude regions of Mars: Journal of Geophysical Research, v. 78, no. 20, p. 4123–4137.

McCauley, J.F., Carr, M.H., Cutts, J.A., Hartmann, W.K., Masursky, Harold, Milton, D.J., Sharp, R.P., and Wilhelms, D.E., 1972, Preliminary Mariner 9 report on the geology of Mars: Icarus, v. 17, no. 2, p. 289–327.

Moore, H.J., Arthur, D.W.G., and Schaber, G.G., 1978, Yield strengths of flows on the Earth, Mars, and Moon, *in* Lunar and Planetary Science Conference, 9th, Houston, March 13–17, 1978, Proceedings: Pergamon Press, p. 3351–3378.

Morris, E.C., 1981, Structure of Olympus Mons and its basal scarp, *in* Third International Colloquium on Mars, LPI Contribution 441: Houston, Lunar and Planetary Institute, p. 161–162.

_____ 1982, Aureole deposits of the Martian volcano Olympus Mons: Journal of Geophysical Research, v. 87, no. B2, p. 1164–1178.

_____ 1987, The "missing" flank of Olympus Mons, Mars, *in* Geological Society of America Annual Meeting and Exposition, Phoenix, Ariz., October 26–29, 1987, Abstracts with Programs, v. 19, no. 7, p. 778–779.

Morris, E.C., Masursky, Harold, Applebee, D.J., and Strobell, M.E., 1991, Geologic maps of Science Study Area 3, Olympus Rupes, Mars (special MTM 15132 quadrangle): U.S. Geological Survey Miscellaneous Investigations Series Map I-2001, 2 sheets, scale 1:500,000.

Morris, E.C., and Dwornik, S.E., 1978, Geologic map of the Amazonis quadrangle of Mars: U.S. Geological Survey Miscellaneous Investigations Series Map I-1049, scale 1:5,000,000.

Morris, E.C., and Howard, K.A., 1981, Geologic map of the Diacria quadrangle of Mars: U.S. Geological Survey Miscellaneous Investigations Series Map I-1286, scale 1:5,000,000.

Mouginis-Mark, P.J., 1981, Late-stage summit activity of martian shield volcanoes, *in* Lunar and Planetary Science Conference, 12th, Houston, March 16–20, 1981, Proceedings: Geochimica et Cosmochimica Acta, v. 12B, p. 1431–1447.

_____ 1990, Recent water release in the Tharsis region of Mars: Icarus, v. 84, no. 2, p. 352–373.

Neal, Christina, 1981, Crater counts on Olympus Mons [abs.], *in* Reports of Planetary Geology Program—1981: National Aeronautics and Space Administration Technical Memorandum 84211, p. 416–418.

Plescia, J.B., and Saunders, R.S., 1979, The chronology of the martian volcanoes, *in* Lunar and Planetary Science Conference, 10th, Houston, March 19–23, 1979, Proceedings: Geochimica et Cosmochimica Acta, p. 2841–2859.

_____ 1982, Tectonic history of the Tharsis region, Mars: Journal of Geophysical Research, v. 87, no. B12, p. 9775–9791.

Rhodes, D.D., and Neal, Christina, 1981, Crescent-shaped pits on Mars, *in* Reports of Planetary Geology Program—1981: National Aeronautics and Space Administration Technical Memorandum 84211, p. 232–234.

Schaber, G.G., Horstman, K.C., and Dial, A.L., Jr., 1978, Lava flow materials in the Tharsis region of Mars, *in* Lunar and Planetary Science Conference, 9th, Houston, March 13–17, 1978, Proceedings: Pergamon Press, p. 3433–3458.

Schiaparelli, G.V., 1879, Osservazioni astronomiche e fisiche sull'asse di rotazione e sulla topografia del pianeta Marte, *in* Atti della R. Accademia dei Lincei, Memoria della cl. di scienze fisiche, ser. 3, v. 10, 387 p.

Schneeberger, D.M., and Pieri, D.C., 1991, Geomorphic-stratigraphic implications for the volcanic history of Alba Patera, Mars: Journal of Geophysical Research, v. 96, no. B2, p. 1907–1930.

Schultz, P.H., and Lutz, A.B., 1988, Polar wandering of Mars: Icarus, v. 73, no. 1, p. 91–141.

Scott, D.H., 1982, Volcanoes and volcanic provinces: Martian western hemisphere: Journal of Geophysical Research, v. 87, no. B12, p. 9839–9851.

Scott, D.H., and Carr, M.H., 1978, Geologic map of Mars: U.S. Geological Survey Miscellaneous Investigations Series Map I-1083, scale 1:25,000,000.

Scott, D.H., and Dohm, J.M., 1990, Faults and ridges: Historical development in Tempe Terra and Ulysses Patera regions of Mars, *in* Lunar and Planetary Science Conference, 20th, Houston, March 13–17, 1989, Proceedings: Lunar and Planetary Institute, p. 503–513.

Scott, D.H., Schaber, G.G., Tanaka, K.L., Horstman, K.C., and Dial, A.L., Jr., 1981, Map series showing lava-flow fronts in the Tharsis region of Mars: U.S. Geological Survey Miscellaneous Investigations Series Maps I-1266 to I-1280, scale 1:5,000,000.

Scott, D.H., and Tanaka, K.L., 1981, Mars: Paleostratigraphic restoration of buried surfaces in Tharsis Montes: Icarus, v. 45, no. 2, p. 304–319.

_____ 1982, Ignimbrites of Amazonis Planitia region of Mars: Journal of Geophysical Research, v. 87, no. B2, p. 1179–1190.

_____ 1986, Geologic map of the western equatorial region of Mars: U.S. Geological Survey Miscellaneous Investigations Series Map I-1082-A, scale 1:15,000,000.

Sjogren, W.L., 1979, Mars gravity: High resolution results from Viking Orbiter 2: Science, v. 203, no. 9, p. 1006–1010.

Solomon, S.C., and Head, J.W., 1982, Evolution of the Tharsis province of Mars: The importance of heterogeneous lithospheric thickness and volcanic construction: Journal of Geophysical Research, v. 87, no. B12, p. 9755–9774.

Squyres, S.W., and Carr, M.H., 1986, Geomorphic evidence for the distribution of ground ice on Mars: Science, v. 231, no. 4735, p. 249–252.

Swanson, D.A., 1972, Magma supply rate at Kilauea volcano 1952–1971: Science, v. 175, no. 4018, p. 169–170.

Tanaka, K.L., 1982, Landslides of Vermillion Cliffs, Arizona: Application to Mars, *in* Reports of Planetary Geology Program—1982: National Aeronautics and Space Administration Technical Memorandum 85127, p. 253–255.

_____1983, Geology of the Olympus Mons region of Mars: Santa Barbara, University of California, Ph.D. dissertation, 264 p., map scale 1:3,000,000.

_____1985, Ice-lubricated gravity spreading of the Olympus Mons aureole deposits: Icarus, v. 62, no. 2, p. 191–206.

_____1986, The stratigraphy of Mars, *in* Lunar and Planetary Science Conference, 17th, Houston, March 17–21, 1986, Proceedings, pt. 1: Journal of Geophysical Research, v. 91, no. B13, p. E139–E158.

_____1990, Tectonic history of the Alba Patera-Ceraunius Fossae region of Mars, *in* Lunar and Planetary Science Conference, 20th, Houston, March 13–17, 1989, Proceedings: Lunar and Planetary Institute, p. 515–523.

Tanaka, K.L., and Davis, P.A., 1988, Tectonic history of the Syria Planum province of Mars: Journal of Geophysical Research, v. 93, no. B12, p. 14,893–14,917.

Tanaka, K.L., Isbell, N.K., Scott, D.H., Greeley, Ronald, and Guest, J.E., 1988, The resurfacing history of Mars: A synthesis of digitized, Viking-based geology, *in* Lunar and Planetary Science Conference, 18th, Houston, March 16–20, 1987, Proceedings: Cambridge University Press and Lunar and Planetary Institute, p. 665–678.

Tanaka, K.L., Scott, D.H., and Greeley, Ronald, 1992, Global stratigraphy, Chapter 11, *in* Kieffer, H.H., Jakosky, B.M., and Snyder, C.W., eds., Mars: Tucson, University of Arizona Press, 1498 p.

Thomas, P.J., Squyres, S.W., and Carr, M.H., 1990, Flank tectonics of Martian volcanoes: Journal of Geophysical Research, v. 95, no. B9, p. 14,345–14,355.

U.S. Geological Survey, 1981, Controlled photomosaic of the Olympus Mons region of Mars: U.S. Geological Survey Miscellaneous Investigations Series Map I–1379, scale 1:2,000,000.

_____1982, Shaded relief map of the western region of Mars: U.S. Geological Survey Miscellaneous Investigations Series Map I–1320, scale 1:15,000,000.

_____1989, Topographic maps of the western, eastern equatorial, and polar regions of Mars: U.S. Geological Survey Miscellaneous Investigations Series Map I–2030, scale 1:15,000,000.

Ward, A.W., 1979, Yardangs on Mars: Evidence of recent wind erosion: Journal of Geophysical Research, v. 84, no. B14, p. 8147–8166.

Wilhelms, D.E., 1987, The geologic history of the Moon: U.S. Geological Survey Professional Paper 1348, 302 p.

Wise, D.U., Golombek, M.P., and McGill, G.E., 1979, Tharsis province of Mars: Geologic sequence, geometry, and a deformation mechanism: Icarus, v. 38, no. 3, p. 456–472.

Wu, S.S.C., Garcia, P.A., Jordan, Raymond, and Schafer, F.J., 1981, Topographic map of Olympus Mons, *in* Third International Colloquium on Mars: Houston, Lunar and Planetary Institute Contribution 441, p. 287–289.

Zuber, M.T., and Mouginis-Mark, P.J., 1990, Constraints on the depth and geometry of the magma chamber of the Olympus Mons volcano, Mars, *in* Abstracts of papers submitted to the Twenty-first Lunar and Planetary Science Conference, Houston, March 12–16, 1990: Lunar and Planetary Institute, p. 1387–1388.

*U.S. G.P.O.:1994-387-030:44